Observable effects of symmetry energy in heavy-ion collisions at intermediate energies

Bao-An Li

Department of Chemistry and Physics, P.O. Box 419, Arkansas State University, State University, Arkansas 72467-0419, USA

Within an isospin-dependent transport model for nuclear reactions induced by neutron-rich nuclei, we perform a comparative study of ^{100}Sn$+^{124}$Sn and ^{100}Zn$+^{124}$Zn reactions at beam energies of 30 MeV/nucleon and 400 MeV/nucleon to identify optimal experimental conditions and observables for investigating the equation of state (EOS) of neutron-rich matter at the Rare Isotope Accelerator (RIA). Several observables known to be sensitive to the density dependence of the symmetry energy are examined as a function of impact parameter for both reaction systems. In particular, the strength of isospin transport/diffusion is studied by using rapidity distributions of free nucleons and their isospin asymmetries. An approximate isospin equilibrium is established even for peripheral collisions with a very soft symmetry energy at 30 MeV/nucleon. At 400 MeV/nucleon, however, a strong isospin translucency is observed even in most central collisions with either soft or stiff symmetry energies. Origins of these observations and their implications to determining the EOS of neutron-rich matter at the RIA are discussed.

The isospin dependence of the nuclear equation of state (EOS) is one of the most important but yet very poorly known properties of neutron-rich matter [1]. Its determination in laboratory-controlled experiments has profound implications to the study of many critical issues in astrophysics [2,3]. Nuclear reactions induced by radioactive beams provide a unique opportunity to extract useful information about the EOS and novel properties of neutron-rich matter. In particular, at the Rare Isotope Accelerator (RIA), heavy ions up to 400 MeV/nucleon will be available. It just enables the study of neutron-rich matter up to about three times normal nuclear matter density. A number of experimental observables have already been identified as sensitive probes of the EOS of neutron-rich matter [4–17]. To gauge the sensitivity of some of these observables in reactions to be available at RIA, we carry out a comparative study of nuclear reactions induced by ^{100}Sn$(N/Z=1)$ and ^{100}Zn$(N/Z=2.3)$ on ^{124}Sn$(N/Z=1.48)$ target at 30 MeV/nucleon and 400 MeV/nucleon from central to peripheral collisions. Results of this study are useful for planning experiments and designing new detectors at RIA. Moreover, the role of isospin degree of freedom in nuclear dynamics at RIA energies is an interesting subject in its own right.

At present, nuclear many-body theories predict vastly different isospin dependence of the nuclear EOS depending on both the calculation techniques and the bare two-body and/or three-body interactions employed, see e.g., Refs. [18–21]. Various theoretical studies (e.g., Refs. [22,23]) have shown that the energy per nucleon $e(\rho,\delta)$ in nuclear matter of density ρ and isospin asymmetry parameter δ defined as $\delta \equiv (\rho_n-\rho_p)/(\rho_n+\rho_p)$ can be approximated very well by a parabolic function $e(\rho,\delta)=e(\rho,0)+E_{sym}(\rho)\delta^2$. In the above, $e(\rho,0)$ is the EOS of isospin symmetric nuclear matter and $E_{sym}(\rho)$ is the symmetry energy at density ρ. We shall use for isospin-symmetric nuclear matter a stiff EOS with $K_0 =380$ MeV which can reproduce the transverse flow data equally well as a momentum-dependent soft EOS with $K_0 =210$ MeV [24,25]. The choice of K_0 does not affect our

conclusions. The EOS of asymmetric matter should also be momentum dependent since both the isoscalar and isovector potentials are momentum dependent [26,27]. For this comparative study, however, it is perfectly sufficient and much more efficient in calculations to use the momentum-independent EOS.

The form of the symmetry energy as a function of density is rather strongly model dependent. We adopt here a parametrization used by Heiselberg and Hjorth-Jensen in their studies on neutron stars [28] $E_{sym}(\rho)=E_{sym}(\rho_0)u^\gamma$, where u
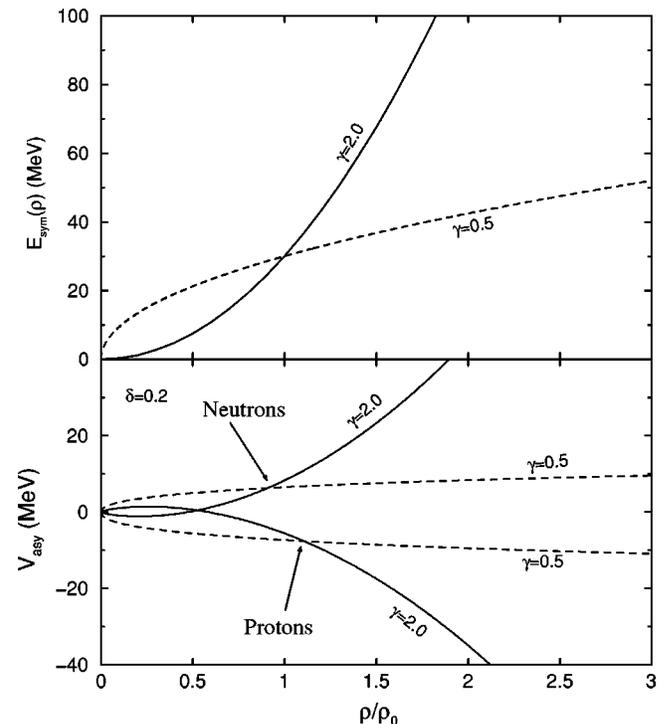

FIG. 1. Symmetry energy (upper window) and symmetry potentials as a function of density for an isospin asymmetry of $\delta=0.2$ and the γ parameter of 0.5 and 2.0, respectively.
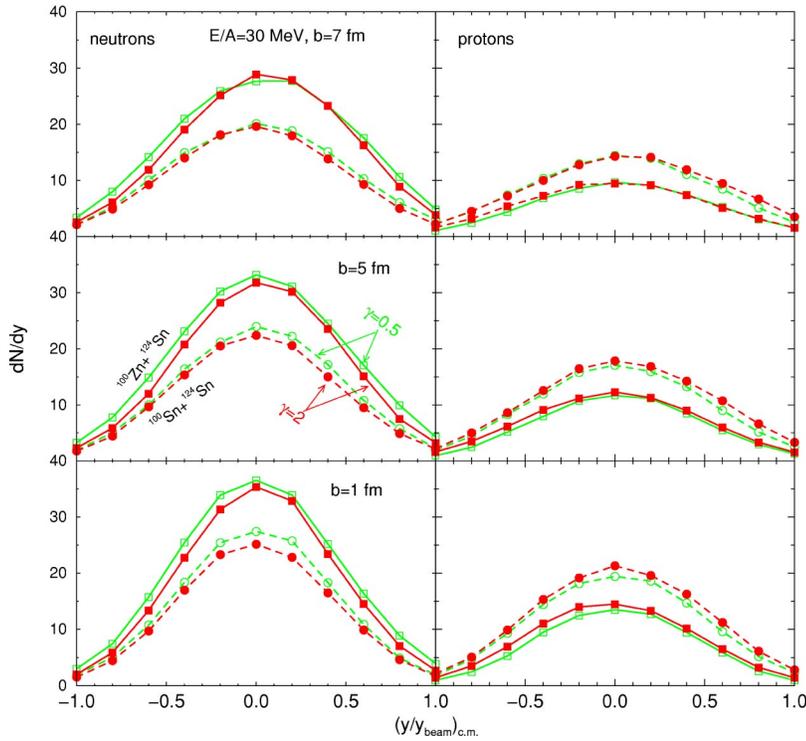
FIG. 2. (Color online) Rapidity distributions of neutrons (left) and protons (right) in the reaction of ^{100}Sn+^{124}Sn and ^{100}Zn+^{124}Sn at a beam energy of 30 MeV/nucleon.

$\equiv \rho/\rho_0$ is the reduced density and $E_{sym}(\rho_0)$ is the symmetry energy at normal nuclear matter density ρ_0. By fitting the result of variational many-body calculations by Akmal *et al.* [19], Heiselberg and Hjorth-Jensen found the values of $E_{sym}(\rho_0) = 32$ MeV and $\gamma = 0.6$. However, as shown by many other authors previously [20,29] using other approaches, the extracted value of γ varies widely, even its sign at supranormal densities is undetermined. In a recent analysis of isospin diffusion in heavy-ion collisions at 50 MeV/nucleon at the NSCL/MSU, some experimental indications of a γ parameter as high as 2 was found [17]. Therefore, in this work we study influence of the symmetry energy on experimental observables by varying the γ parameter between 0.5 and 2. Assuming no momentum dependence, the corresponding symmetry potentials can be derived directly from the density-dependent symmetry energy [11]. Shown in Fig. 1 are the symmetry
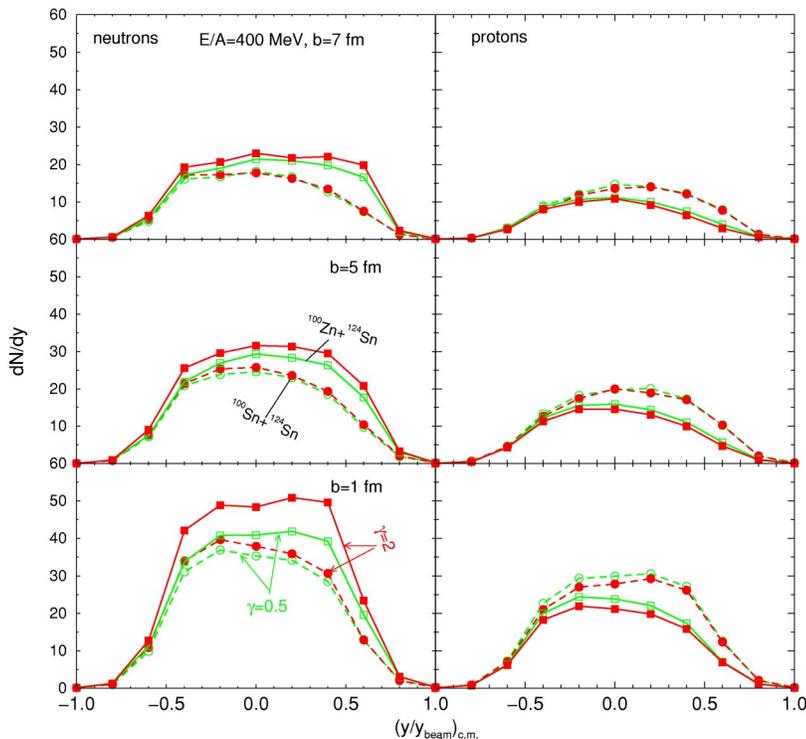

FIG. 3. (Color online) Rapidity distributions of neutrons (left) and protons (right) in the reaction of ^{100}Sn+^{124}Sn and ^{100}Zn+^{124}Sn at a beam energy of 400 MeV/nucleon.
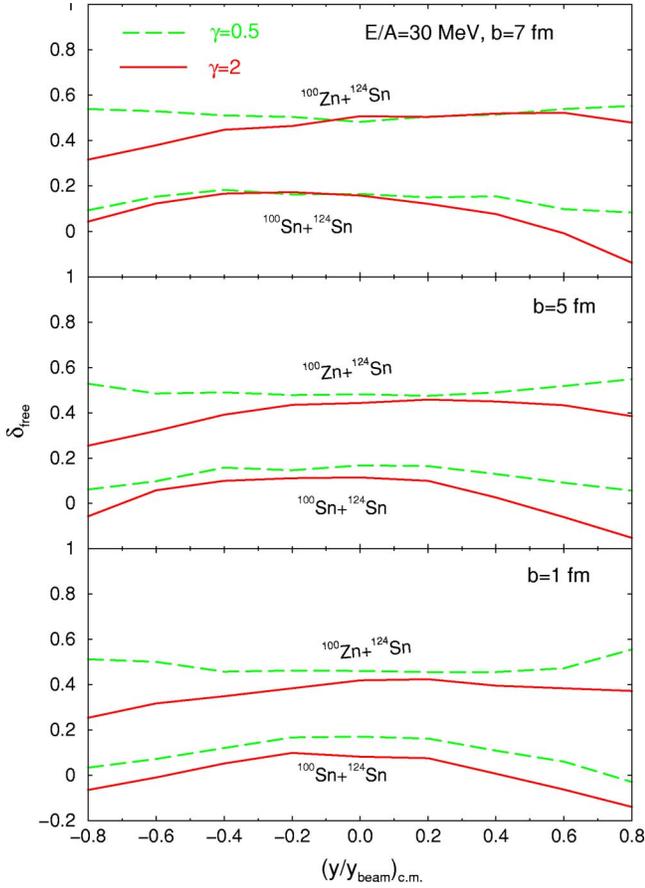
FIG. 4. (Color online) Rapidity distributions of isospin asymmetry of free nucleons in the reaction of ^{100}Sn+^{124}Sn and ^{100}Zn + ^{124}Sn at a beam energy of 30 MeV/nucleon.

FIG. 5. (Color online) Rapidity distributions of isospin asymmetry of free nucleons in the reaction of ^{100}Sn+^{124}Sn and ^{100}Zn + ^{124}Sn at a beam energy of 400 MeV/nucleon.

energy (upper window) and symmetry potentials (lower window) at δ=0.2 as a function of density. It is seen that the soft (γ=0.5) symmetry energy leads to a larger (smaller) magnitude of the symmetry potential than the stiff one (γ=2) at densities below (above) about ρ_0. Since the magnitude of the generally repulsive (attractive) symmetry potential for neutrons (protons) affects significantly the n/p ratio of emitted nucleons, the stiffness of the symmetry energy is thus expected to affect the isospin asymmetry of emitted free nucleons differently at low and high energies. To investigate the density dependence of the symmetry, energy reactions with a broad range of beam energies are useful.

Our study is based on an isospin-dependent Boltzmann-Uehling-Uhlenbeck (IBUU) transport model (e.g., Refs. [11,4,30]). We select ^{100}Sn and ^{100}Zn on the opposite boundaries of stability of mass number 100 as projectiles on a stable ^{124}Sn target. The initial neutron and proton density distributions of the projectile nuclei were calculated by using the Hartree-Fock-Bogoliubov method and were provided to us by Dobaczewski [31]. With these choices the ^{100}Sn + ^{124}Sn reaction is symmetric (highly asymmetric) in protons (neutrons) in the projectile and target, while the ^{100}Zn + ^{124}Sn reaction is approximately symmetric (highly asymmetric) in neutrons (protons). Comparing rapidity distributions of neutrons (protons), for instance, of these two reac-
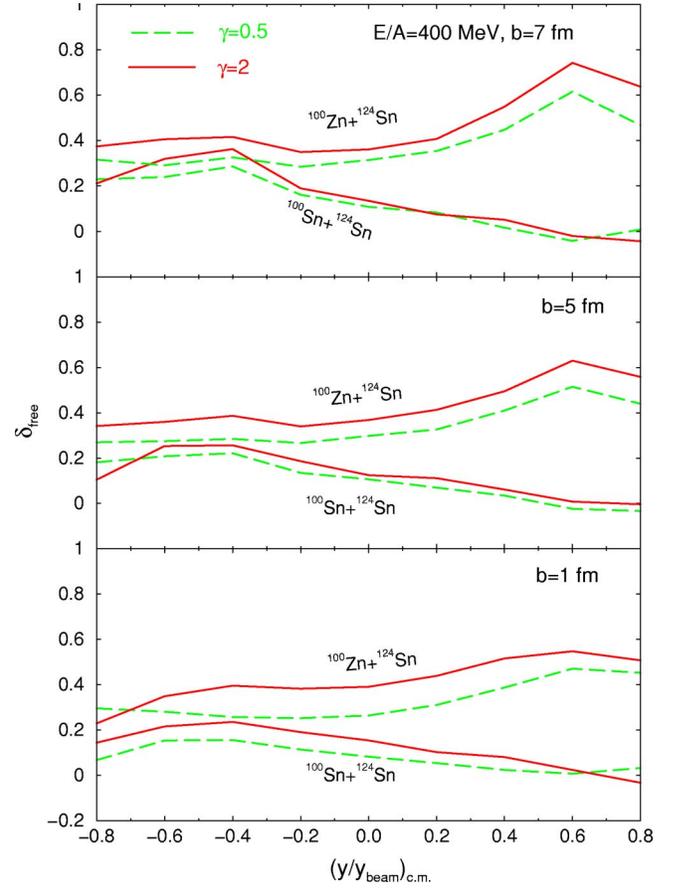
tions will allow us to investigate the isospin transport and possible isospin equilibration.

Shown in Fig. 2 and 3 are the distributions of free neutrons (left panels) and protons (right panels) as a function of scaled rapidity at a beam energy of 30 MeV/nucleon and 400 MeV/nucleon, respectively, at an impact parameter of 1, 5, and 7 fm. Here we have selected free nucleons as those having local densities less than $\rho_0/8$ at freeze-out.

First of all, it is seen that at 30 MeV/nucleon the rapidity distributions of both neutrons and protons are about symmetric around $(y/y_{beam})_{cm}$=0, indicating a high degree of isospin and kinetic equilibrium. At 400 MeV/nucleon, however, distinct forward/backward asymmetries are seen in the rapidity distributions of neutrons in ^{100}Sn+^{124}Sn and protons in ^{100}Zn+^{124}Sn even in the most central collisions, indicating a significant nuclear translucency and nonstopping. Second, the main effect of the generally repulsive (attractive) symmetry potential for neutrons (protons) is to cause more (less) neutrons (protons) to become free. This effect relies directly on the magnitude of the symmetry potential. At 30 MeV/nucleon, since the symmetry potential is higher with γ=0.5 than with γ=2 as shown in Fig. 1, there are thus more (less) free neutrons (protons) emitted with γ=0.5 than with γ=2. While the opposite is true at 400 MeV/nucleon since the magnitude of the symmetry potential reverses its order above ρ_0 with γ=2 leading to higher symmetry potentials now.
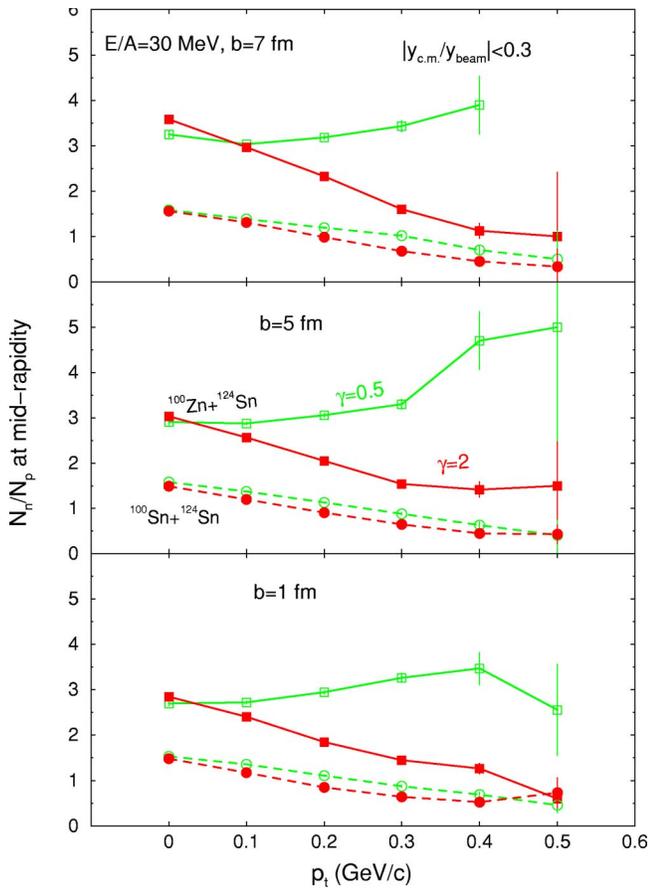
FIG. 6. (Color online) Transverse momentum dependence of the neutron/proton ratio at midrapidity for the reaction of ^{100}Sn $+^{124}$Sn and ^{100}Zn$+^{124}$Sn at a beam energy of 30 MeV/nucleon.

FIG. 7. (Color online) Transverse momentum dependence of the neutron/proton ratio at midrapidity for the reaction of ^{100}Sn $+^{124}$Sn and ^{100}Zn$+^{124}$Sn at a beam energy of 400 MeV/nucleon.

To be more quantitative about the degree of isospin equilibrium and to examine effects of the symmetry potential on isospin transport, we show in Fig. 4 and 5 the isospin asymmetry of free nucleons as a function of rapidity. It is seen that a rather uniform isospin asymmetry is achieved over the whole rapidity range only with $\gamma=0.5$ at 30 MeV/nucleon because of the large magnitude of the symmetry potential at densities relevant to the reaction. At 400 MeV/nucleon, an appreciable backward-forward asymmetric isospin asymmetry exists for both reactions. With $\gamma=2$ the overall isospin asymmetry of free nucleons are significantly higher than that with $\gamma=0.5$. This is what one expects based on the density dependence of the symmetry potential shown in Fig. 1. Moreover, in contrast to the case at 30 MeV/nucleon, the reaction time at 400 MeV/nucleon is much too short compared to the time necessary for the system to reach the global isospin equilibrium [32,33].

A good quantitative measure of the isospin transport is the neutron to proton ratio at midrapidity. Shown in Fig. 6 and Fig. 7 are the n/p ratios at midrapidity versus the transverse momentum p_t at 30 MeV/nucleon and 400 MeV/nucleon, respectively. For the neutron-rich system ^{100}Zn$+^{124}$Sn at low transverse momenta at both beam energies, the n/p ratio is obviously increased compared to that of the reaction system. At both energies there is a general trend of an increasing n/p ratio at lower transverse momenta, except the case of γ
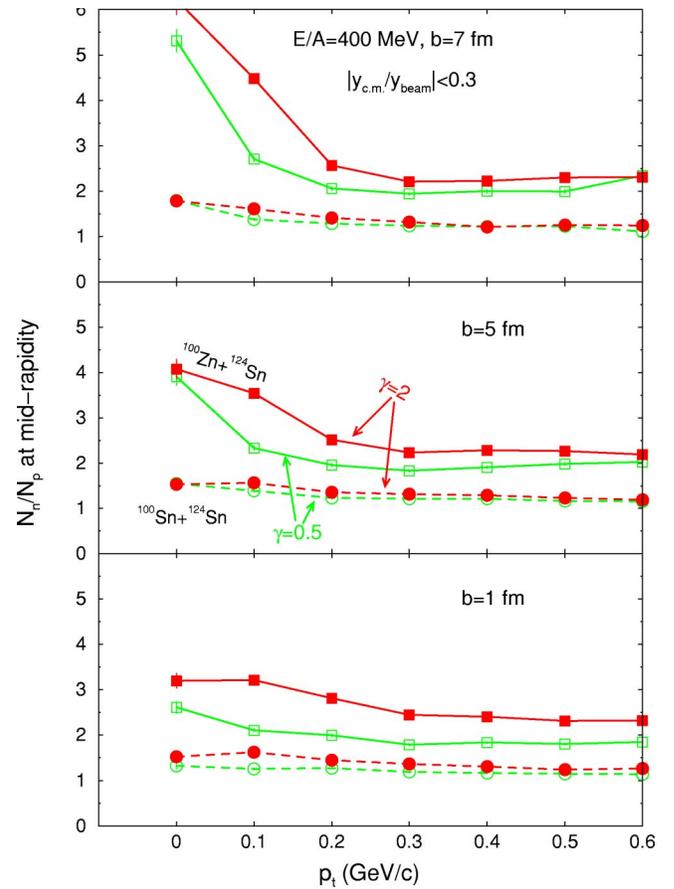
=0.5 at 30 MeV/nucleon. This trend is mainly due to the Coulomb effect which shifts protons from low energies to higher energies. While the generally attractive symmetry potential for protons works against the Coulomb potential. For protons at low transverse momenta the Coulomb potential dominates. While at higher transverse momenta with the parameter $\gamma=0.5$ the symmetry potential dominates. With the soft symmetry energy at 30 MeV/nucleon, the n/p ratio reaches the highest value at the highest transverse momentum. There is thus a strong sensitivity to the symmetry energy at high transverse momenta at 30 MeV/nucleon. The n/p ratio differs by more than a factor of 2 by using $\gamma=0.5$ and $\gamma=2$. This is mainly due to the fact that these high transverse momentum nucleons have gone through regions of higher density gradients.

At 400 MeV/nucleon, effect of the symmetry potential is still obvious but not as dramatic as that at 30 MeV/nucleon. Two effects are responsible for this observation. First, mean field effects are weaker at higher energies than at lower energies. Second, because of the particular functional form of the symmetry potential used here, the relative strengthes of the symmetry potentials are just opposite at supranormal and subnormal densities with $\gamma=0.5$ and 2 as shown in Fig. 1. At 30 MeV/nucleon, only the low-density part up to about 1.2 ρ_0 contributes while at 400 MeV/nucleon a broad range of densities up to about 3 ρ_0 is involved. Of course, at
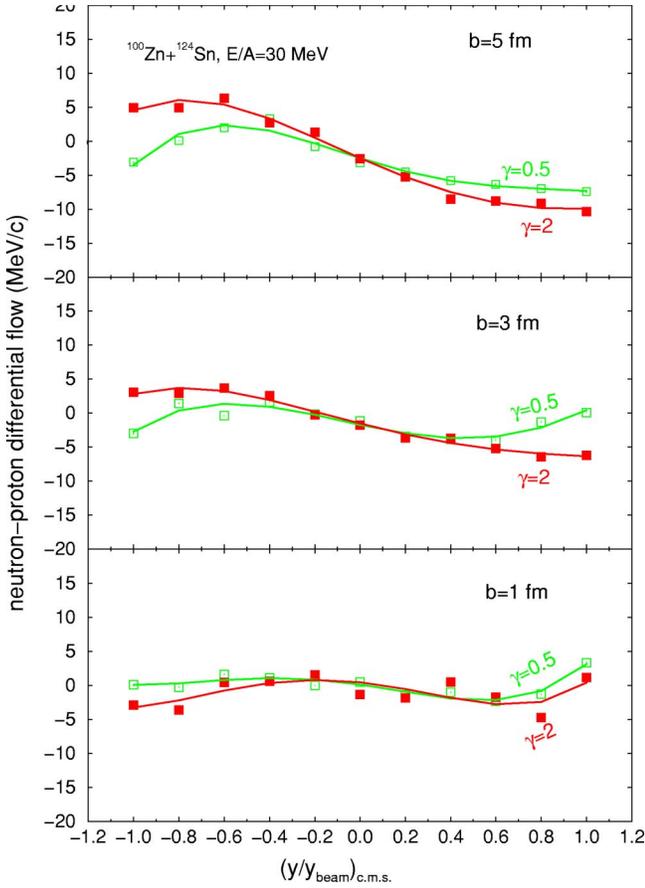
FIG. 8. (Color online) Neutron-proton differential flow for the reaction of ^{100}Zn+^{124}Sn at a beam energy of 30 MeV/nucleon.

FIG. 9. (Color online) Neutron-proton differential flow for the reaction of ^{100}Zn+^{124}Sn at a beam energy of 400 MeV/nucleon.

400 MeV/nucleon effects of the high-density region dominate although there is a concealing effect for particles going through both low- and high-density regions. Thus the n/p ratio is higher with $\gamma=2$ than with $\gamma=0.5$ in contrast to the 30 MeV/nucleon case. Therefore, the midrapidity n/p ratio observable is mostly useful for learning the symmetry energy at subnormal densities in reactions with beam energies around the Fermi energy. We shall discuss in the following two observables that are more useful for learning the symmetry energy at supranormal densities in reactions at higher beam energies.

We now examine the neutron-proton differential flow for the neutron-rich system ^{100}Zn+^{124}Sn. The neutron-proton differential flow in neutron-deficient reactions is not sensitive to the symmetry energy as one expects. The neutron-proton differential flow is defined as

$$F_{n-p}^{x}(y) \equiv \sum_{i=1}^{N(y)} (p_i^x w_i)/N(y), \qquad (1)$$

where $w_i=1(-1)$ for neutrons (protons) and $N(y)$ is the total number of free nucleons at rapidity y. It combines constructively effects of the symmetry potential on the isospin fractionation and the collective flow. It also has the advantage of maximizing effects of the symmetry potential while minimizing effects of the isoscalar potential [12]. Shown in Fig. 8
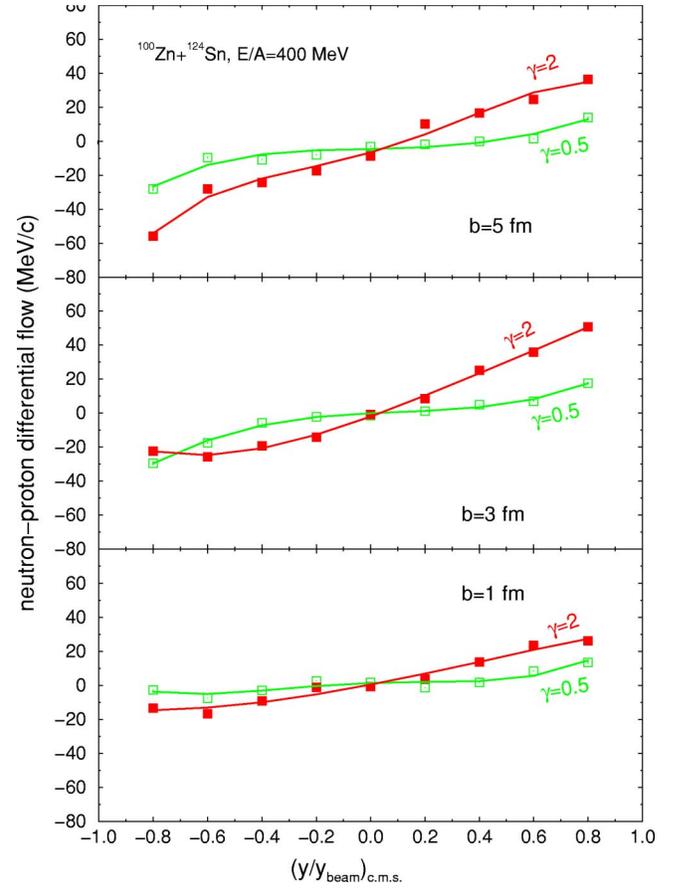
and Fig. 9 are the neutron-proton differential flows in central and midcentral collisions at 30 MeV/nucleon and 400 MeV/nucleon, respectively.

At 30 MeV/nucleon, one observes an antiflow while at 400 MeV/nucleon there is a positive flow. This transition from negative to positive flow from the Fermi energy to relativistic energies is well known [34]. At both energies there is clearly an observable symmetry energy effect. Again, the higher magnitude of symmetry potential at low densities with $\gamma=0.5$ and at higher densities with $\gamma=2$ leads to the higher neutron-proton differential flow at 30 MeV/nucleon and 400 MeV/nucleon, respectively. Obviously the symmetry energy effect is now much stronger at 400 MeV/nucleon than at 30 MeV/nucleon. This is consistent with the well-known finding that the transverse flow is sensitive to the early density and pressure gradients [3]. Therefore, the neutron-proton differential flow is more useful for studying the symmetry energy at high densities.

Another observable known to be sensitive to the high-density behavior of symmetry energy is the π^-/π^+ ratio [14,35]. Shown in Fig. 10 are the π^-/π^+ ratios at 400 MeV/nucleon from central to peripheral collisions. It is seen that the π^-/π^+ ratio is sensitive to both the n/p ratio of the reaction system and the symmetry energy, especially in central collisions. As discussed in detail in Refs. [14,35], the π^-/π^+ ratio is sensitive to the isospin asymmetry of the high-density region $(n/p)_{dense}$. While the latter is determined
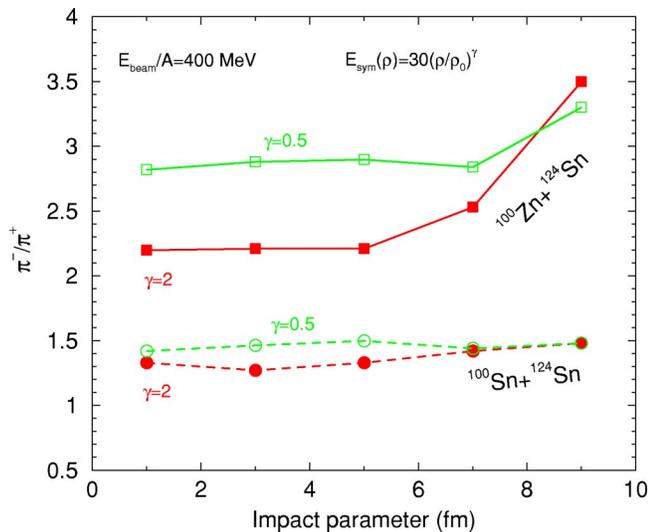
FIG. 10. (Color online) π^-/π^+ ratio as a function of impact parameter in the reaction of ^{100}Zn+^{124}Sn at a beam energy of 400 MeV/nucleon.

by the stiffness of the symmetry energy. The soft symmetry energy at supranormal densities favors the formation of a neutron-rich high-density region and a neutron-deficit low-density region. In our discussions above, it has been shown that at 400 MeV/nucleon with $\gamma=0.5$ the n/p ratios of free nucleons are less than those with $\gamma=2$. Thus the corresponding $(n/p)_{dense}$ and π^-/π^+ ratios are higher with $\gamma=0.5$. It is seen from Fig. 10 that the π^-/π^+ ratio is about 25% higher with $\gamma=0.5$ than with $\gamma=2$ in central collisions.

In summary, within an isospin-dependent transport model for nuclear reactions induced by neutron-rich nuclei, we carried out a comparative study of ^{100}Sn+^{124}Sn and ^{100}Zn +^{124}Sn reactions at a beam energy of 30 MeV/nucleon and 400 MeV/nucleon, respectively. The strength of isospin transport/diffusion is studied by using the rapidity distributions of free nucleons and their isospin asymmetries. An approximate isospin equilibrium can be obtained even for peripheral collisions with only the soft symmetry energy at 30 MeV/nucleon. At 400 MeV/nucleon, however, an appreciable isospin translucency happens even in the most central collisions. We found that the neutron/proton ratio at midrapidity but high transverse momenta at 30 MeV/nucleon is most sensitive to the symmetry energy at subnormal densities. On the other hand, at higher beam energies, e.g., 400 MeV/nucleon, neutron-proton differential flow and the π^-/π^+ ratio are found to be more sensitive to the density dependence of the symmetry energy at supranormal densities. To map out the entire density dependence of the symmetry energy a combination of several complementary observables in a broad range of beam energies is necessary. These observations are useful for planning experiments and designing new detectors for exploring the EOS of neutron-rich matter at RIA. Several observables useful for studying the EOS of neutron-rich matter require the detection of neutrons.

[1] *Isospin Physics in Heavy-Ion Collisions at Intermediate Energies*, edited by B. A. Li and W. Udo Schröder (Nova Science, New York, 2001).

[2] J. M. Lattimer and M. Prakash, Phys. Rep. **333**, 121 (2000).

[3] P. Danielewicz, R. Lacey, and W. G. Lynch, Science **298**, 1592 (2002).

[4] B. A. Li, C. M. Ko, and Z. Z. Ren, Phys. Rev. Lett. **78**, 1644 (1997).

[5] B. A. Li and C. M. Ko, Nucl. Phys. **A618**, 498 (1997).

[6] V. Baran, M. Colonna, M. Di Toro, and A. B. Larionov, Nucl. Phys. **A632**, 287 (1998).

[7] H. S. Xu *et al.*, Phys. Rev. Lett. **85**, 716 (2000).

[8] W. P. Tan *et al.*, Phys. Rev. C **64**, 051901(R) (2001).

[9] V. Baran, M. Colonna, M. Di Toro, V. Greco, and M. Zielinska-Pfabé, and H. H. Wolter, Nucl. Phys. **A703**, 603 (2002).

[10] M. B. Tsang *et al.*, Phys. Rev. Lett. **86**, 5023 (2001).

[11] B. A. Li, A. T. Sustich, and B. Zhang, Phys. Rev. C **64**, 054604 (2001).

[12] B. A. Li, Phys. Rev. Lett. **85**, 4221 (2000).

[13] V. Greco, V. Baran, M. Colonna, M. Di Toro, T. Gaitanos, and H. H. Wolter, Phys. Lett. B **562**, 215 (2003).

[14] B. A. Li, Phys. Rev. Lett. **88**, 192701 (2002); Nucl. Phys. **A708**, 365 (2002).

[15] L. W. Chen, V. Greco, C. M. Ko, and B. A. Li, Phys. Rev. Lett. **90**, 162701 (2003); Phys. Rev. C **68**, 014605 (2003).

[16] L. W. Chen, C. M. Ko, and B. A. Li, Phys. Rev. C **68**, 017601 (2003); Nucl. Phys. **A729**, 809 (2003).

[17] M. B. Tsang *et al.*, Phys. Rev. Lett. (to be published), nucl-ex/ 0310024.

[18] R. B. Wiringa, V. Fiks, and A. Fabrocini, Phys. Rev. C **38**, 1010 (1988).

[19] A. Akmal and V. R. Pandharipande, Phys. Rev. C **56**, 2261 (1997); A. Akmal, V. R. Pandharipande, and D. C. Ravenhall, *ibid.* **58**, 1804 (1998).

[20] B. A. Brown, Phys. Rev. Lett. **85**, 5296 (2000).

[21] C. J. Horowitz *et al.*, Phys. Rev. C **63**, 025501 (2001).

[22] I. Bombaci and U. Lombardo, Phys. Rev. C **44**, 1892 (1991).

[23] H. Huber, F. Weber, and M. K. Weigel, Phys. Lett. B **317**, 485 (1993); Phys. Rev. C **50**, R1287 (1994).

[24] Q. Pan and P. Danielewicz, Phys. Rev. Lett. **70**, 2062 (1993).

[25] J. Zhang, S. Das Gupta, and C. Gale, Phys. Rev. C **50**, 1617 (1994).

[26] C. B. Das, S. Das Gupta, C. Gale, and B. A. Li, Phys. Rev. C **67**, 034611 (2003).

[27] B. A. Li, C. B. Das, S. Das Gupta, C. Gale, Phys. Rev. C **69**, 011603 (2004); Nucl. Phys. A (to be published), nucl-th/ 0312054.

[28] H. Heiselberg and M. Hjorth-Jensen, Phys. Rep. **328**, 237 (2000).

[29] I. Bombaci, in *Isospin Physics in Heavy-Ion Collisions at Intermediate Energies* (Ref. [1]), Chap. 2.

[30] B. A. Li, C. M. Ko, and W. Bauer, Int. J. Mod. Phys. E **7**, 147 (1998).

[31] J. Dobaczewski, Acta Phys. Pol. B **30**, 1647 (1999).

[32] B. A. Li and S. J. Yennello, Phys. Rev. C **52**, R1746 (1995).

[33] B. A. Li and C. M. Ko, Phys. Rev. C **57**, 2065 (1998).

[34] G. D. Westfall, Nucl. Phys. **A630**, 27c (1998), and references therein.

[35] B. A. Li, Phys. Rev. C **67**, 017601 (2003).